Physics Letters B 748 (2015) 89–94

Contents lists available at ScienceDirect

Physics Letters B

www.elsevier.com/locate/physletb

Excitation energy dependence of fragment-mass distributions from fission of ^{180,190}Hg formed in fusion reactions of ^{36}Ar + ^{144,154}Sm

K. Nishio [a,*], A.N. Andreyev [a,b,c], R. Chapman [c], X. Derkx [d,e], Ch.E. Düllmann [d,f,e], L. Ghys [g,h], F.P. Heßberger [f,e], K. Hirose [a], H. Ikezoe [a], J. Khuyagbaatar [e,f], B. Kindler [f], B. Lommel [f], H. Makii [a], I. Nishinaka [a], T. Ohtsuki [i], S.D. Pain [c,j], R. Sagaidak [k], I. Tsekhanovich [l], M. Venhart [g], Y. Wakabayashi [a,m], S. Yan [n]

[a] Advanced Science Research Center, Japan Atomic Energy Agency, Tokai, Ibaraki 319-1195, Japan
[b] Department of Physics, University of York, Heslington, York, YO10 5DD, United Kingdom
[c] School of Engineering, The University of the West of Scotland, Paisley Campus, High Street, Paisley, Renfrewshire, United Kingdom
[d] Institute of Nuclear Chemistry, Johannes Gutenberg University Mainz, 55128 Mainz, Germany
[e] Helmholtz Institute Mainz, 55099 Mainz, Germany
[f] GSI Helmholtzzentrum für Schwerionenforschung, 64291 Darmstadt, Germany
[g] KU Leuven, Instituut voor Kern-en Stralighsfysica, 3001 Leuven, Belgium
[h] Belgian Nuclear Research Center SCK•CEN, Boeretang 200, B-2400 Mol, Belgium
[i] Research Reactor Institute, Kyoto University, Osaka 590-0494, Japan
[j] Oak Ridge National Laboratory, Oak Ridge, TN 37831, USA
[k] Flerov Laboratory of Nuclear Reactions, Joint Institute for Nuclear Research, RU-141980, Dubna, Russia
[l] University of Bordeaux, 351 cours de la Libération 33405 Talence Cedex, France
[m] RIKEN, Nishina-Center, Wako 351-0198, Japan
[n] China Institute of Atomic Energy, P.O. Box 275(10), Beijing, China

ARTICLE INFO

Article history:
Received 11 April 2015
Received in revised form 10 June 2015
Accepted 27 June 2015
Available online 30 June 2015
Editor: V. Metag

Keywords:
^{180,190}Hg
Fusion–fission
Mass asymmetric fission

ABSTRACT

Mass distributions of fission fragments from the compound nuclei ^{180}Hg and ^{190}Hg formed in fusion reactions ^{36}Ar + ^{144}Sm and ^{36}Ar + ^{154}Sm, respectively, were measured at initial excitation energies of $E^*(^{180}\text{Hg}) = 33$–$66$ MeV and $E^*(^{190}\text{Hg}) = 48$–$71$ MeV. In the fission of ^{180}Hg, the mass spectra were well reproduced by assuming only an asymmetric-mass division, with most probable light and heavy fragment masses $\bar{A}_L/\bar{A}_H = 79/101$. The mass asymmetry for ^{180}Hg agrees well with that obtained in the low-energy β^+/EC-delayed fission of ^{180}Tl, from our earlier ISOLDE(CERN) experiment. Fission of ^{190}Hg is found to proceed in a similar way, delivering the mass asymmetry of $\bar{A}_L/\bar{A}_H = 83/107$, throughout the measured excitation energy range. The persistence as a function of excitation energy of the mass-asymmetric fission for both proton-rich Hg isotopes gives strong evidence for the survival of microscopic effects up to effective excitation energies of compound nuclei as high as 40 MeV. This behavior is different from fission of actinide nuclei and heavier mercury isotope ^{198}Hg.

1. Introduction

A predominantly asymmetric mass distribution (MD) of fission fragments (FFs) observed in spontaneous fission or in low-energy induced fission of actinide nuclei is usually attributed to the effects of shell structure of the fissioning parent nucleus or final FFs. Consequently, the asymmetry in the masses of fragments is believed to be governed by spherical shell closures in the vicinity of ^{132}Sn ($N = 82$, $Z = 50$) or/and by deformed neutron shells (e.g., $N = 88$) [1]. Contrary to actinides, the low-energy fission of nuclei around ^{208}Pb (e.g. ^{212}Po) was found to produce a symmetric FFs mass distribution [2]. Some nuclides between the lead and actinide regions are known to have intermediate properties, which is reflected in a triple-humped structure of the mass distribution, arising from contributions of both symmetric and asymmetric mass splits [3,4]. This was further confirmed for some of the neutron-deficient At–Ac ($85 \leq Z \leq 89$) isotopes using Coulomb excitation of relativistic radioactive beams in inverse kinematics at GSI [5].

* Corresponding author.
E-mail address: nishio.katsuhisa@jaea.go.jp (K. Nishio).

http://dx.doi.org/10.1016/j.physletb.2015.06.068

The FFs mass distribution have also been studied for lighter elements (Ir–At, $77 \leq Z \leq 85$) in the vicinity of ^{208}Pb [6–9]. This is an interesting region of nuclei as far as the fission is concerned, which is characterized by a shorter saddle-to-scission distance in comparison to the heavy actinides. For example, a flat-top mass distribution was found for ^{198}Hg, ^{210}Po, ^{207}Bi, and some other nuclei [6,7], whereas for ^{201}Tl a dip in the mass distribution has been observed for symmetric mass divisions, at the excitation energies of 7–10 MeV above the top of the fission barrier, thus forming an apparently-looking double-peaked structure [6]. A small dip can also be guessed in the MD of ^{198}Hg measured at the excitation energy of 7.4 MeV [6].

Recently, fission of the proton-rich nucleus ^{180}Hg ($Z = 80$, $N = 100$) was investigated via the mechanism of the β^+/EC-delayed fission (βDF) of ^{180}Tl [10,11]. This is a unique system, with a low neutron-to-proton ratio of $N/Z = 1.25$, which is very different from typical values of $N/Z \sim 1.55$ in the heavy actinide region. Also the saddle point of ^{180}Hg is expected to have a much more elongated shape in comparison with that for the actinide nuclei. Already these peculiarities suggest the ^{180}Hg nucleus as an interesting system to study with respect to fission, in which unusual behavior might appear. Furthermore, the mechanism of βDF limits the maximum excitation energy $E^*_{\max}(^{180}\text{Hg})$ of the fissioning daughter ^{180}Hg to Q_{EC} (^{180}Tl) = 10.8 MeV [12], defining the process as the low-energy fission, in which shell effects are expected to be preserved. However, in contrast to the initial anticipation for the system to split symmetrically into two semi-magic ^{90}Zr ($Z = 40$, $N = 50$) fragments, the ^{180}Hg nucleus showed a clearly pronounced mass-asymmetric fission, by generating FFs with most probable masses around $\bar{A}_L = 80(1)$ and $\bar{A}_H = 100(1)$.

The excitation energy dependence of the mass yields is another important aspects in fission studies. For actinide nuclei, it is known experimentally that the asymmetric FFs mass distribution, observed at the low excitation energy, changes to a single-Gaussian shape [13] with increasing excitation energy of a compound nucleus. As another example, a triple-humped FF mass distribution in the radium region also transits into a simple symmetric-fission mass curve with the increase of E^* [14]. Such behavior is interpreted as being due to a weakening of the shell effects with growing excitation. However, the quantitative understanding of the shell damping as a function of excitation energy is still an open problem [15,16].

In this letter, we report on the experimental study of the FFs mass distributions, and their dependence on excitation energy, for the compound nuclei of ^{180}Hg and ^{190}Hg populated in fusion reactions of ^{36}Ar + ^{144}Sm and ^{36}Ar + ^{154}Sm, respectively. The ^{190}Hg nucleus lies between ^{180}Hg, which fissions asymmetrically at low energy, and ^{198}Hg, which fissions symmetrically [6,7], thus allowing the systematic trends to be established in the FFs mass distribution for a long chain of proton-rich mercury isotopes. Our earlier data for ^{180}Hg resulted in a series of calculations of mass yields and their energy dependence performed by different theory groups, see e.g. [17–23]. A comparison of the new data for fusion–fission reactions leading to ^{180,190}Hg with the respective predictions will also be done in the present work.

2. Experimental setup

An ^{36}Ar beam of ~2 pnA in intensity, at several beam energies in the range of 148–198 MeV, was supplied by the tandem accelerator of Japan Atomic Energy Agency (JAEA). The ^{144,154}Sm targets were made by sputtering enriched ^{144,154}Sm materials (samarium fluoride) on 35 μg/cm^2 carbon foils. Isotopic abundances were 93.8% (^{144}Sm) and 98.9% (^{154}Sm). The typical thickness of the target layers was 70 μg/cm^2.

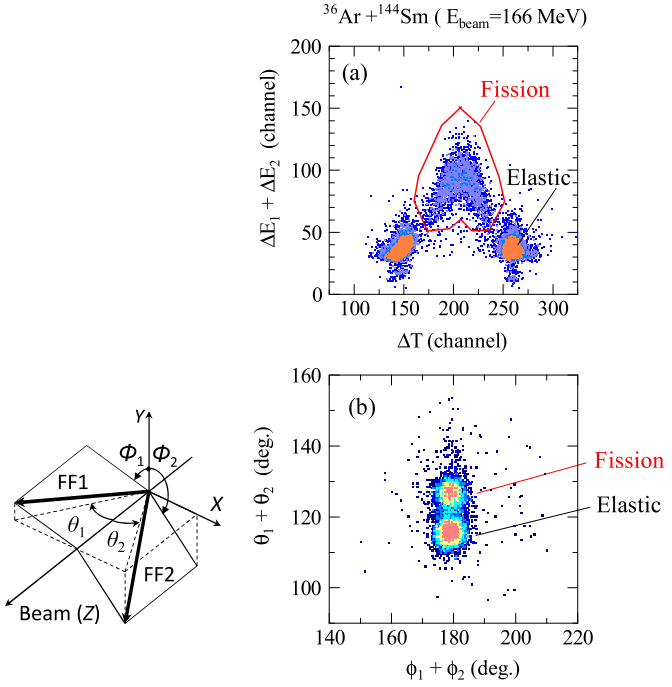

Fig. 1. (Color online.) (left) Definition of emission angles θ_1 and θ_2 and out-of-plane angles ϕ_2 and ϕ_2. (a) Events from the ^{36}Ar + ^{144}Sm reaction, mapped on the ΔE_1+ΔE_2 vs ΔT axes. Fission events within the polygon and elastic-recoil events are clearly separated. (b) Same as in (a) but in the coordinates $\theta_1 + \theta_2$ vs $\phi_1 + \phi_2$.

The experimental setup used in the present work was similar to that described in Ref. [24]. The target was mounted with the carbon backing facing the incoming beam. Both FFs were detected in coincidence using position-sensitive multi-wire proportional counters (MWPCs). The MWPCs have an active area of 200 mm (horizontal) × 120 mm (vertical). The emission angles θ_1 and θ_2 of FF1 and FF2 projected on the X–Z plane and the out-of-plane angles ϕ_1 and ϕ_2 were measured as defined in Fig. 1 (left). The detectors were located symmetrically around the beam axis(Z) at $\theta_1 = -71°$ for MWPC1 and $\theta_2 = +71°$ for MWPC2. The distance between the target and the center of the cathodes was 211 mm. Each MWPC covered emission angles of ±25° around the detector center. For the out-of-plane angles, each MWPC covered the range of $72° \leq \phi_i \leq 108°$ ($i = 1, 2$) at the detector center.

The detectors were operated with isobutane gas at a pressure of about 3 Torr. A 2 μm Mylar film coated with aluminum layer was used as the entrance window.

The time difference ΔT was measured between the two fragments, with start and stop signals obtained from MWPC2 and MWPC1, along with the charges ΔE_1 and ΔE_2 induced in both MWPCs by passing nuclei. These charges are proportional to the energy deposited by the nuclei in the active detector area. Fig. 1 (a) gives an example of measured coincident events in the $\Delta E_1 + \Delta E_2$ vs ΔT coordinate plane, for the ^{36}Ar + ^{144}Sm reaction at the incident beam energy of $E_{\text{beam}} = 166$ MeV. A clear separation between FFs and scattered projectile and recoiled nuclei can be noted. A comparable separation of fission and scattered/recoiled nuclei was obtained for the other incident beam energies.

An additional way to distinquish FFs from the scattered projectile and recoiled nuclei is to exploit the difference in the reactions' kinematics. This is demonstrated in Fig. 1 (b), where events are plotted in the $\theta_1 + \theta_2$ vs $\phi_1 + \phi_2$ coordinate plane, with angles determined from the incident positions in the two MWPCs.

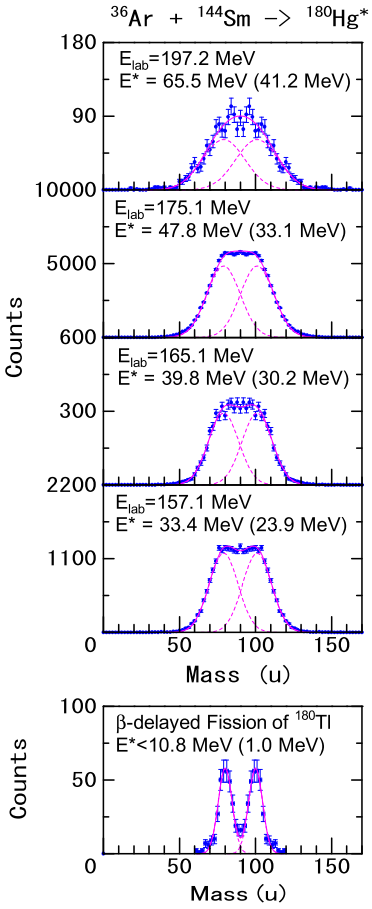

Fig. 2. (Color online.) Fragment-mass distributions from fission of ^{180}Hg at different beam energies $E_{\rm lab}$ obtained in the ^{36}Ar + ^{144}Sm reaction. Excitation energies E^* are also indicated. The effective excitation energy above the fission barrier $E^*_{\rm Eff,B_{f,\langle l\rangle}}$ (see text) is also shown in parentheses. Solid curves are the results of fitting by assuming only a single asymmetric fission mode; the deconvolution between the light- and heavy-mass FFs is shown by dashed curves. Bottom panel: results from the βDF of ^{180}Tl ($E^*(^{180}{\rm Hg}) < 10.8$ MeV) from [10,11].

Calibration for the time difference ΔT was made from the elastic-recoil peak positions appearing in the ΔT spectrum. The timing resolution of ΔT was determined to be $\sigma_{\Delta T} = 0.7$ ns. FFs kinetic energies and masses were then deduced from the kinematic considerations as explained in Ref. [24]. The experimental mass resolution was obtained from the elastic scattering peak and amounted to $\sigma_{\rm m,exp} = 2.4$ u. The precision on the sum energy of elastically scattered projectiles and recoiled nuclei was estimated to be $\sigma_{\rm ela+rec} = 8.6$ MeV.

3. Experimental results

The upper four panels in Fig. 2 show the FFs mass distributions obtained in the reaction ^{36}Ar + ^{144}Sm → ^{180}Hg* at four beam energies in the laboratory frame, $E_{\rm lab}$, corresponding to the middle of the target layer. The energy loss of the beam particles in the carbon backing and the target layer was calculated with the code SRIM [25]. Corresponding excitation energies E^* are also provided, calculated from nuclear masses and beam energies. The indicated errors are the statistical ones corresponding to the 1σ level.

For comparison, the result from the βDF of ^{180}Tl [11], where the daughter ^{180}Hg (after β decay of ^{180}Tl) is the fissioning nucleus, is also shown in the bottom panel in Fig. 2.[1] The measured mass spectrum could be well described with a sum of two Gaussian functions:

$$Y(A) = a\exp\left(-(A-\bar{A}_{\rm L})/2\sigma_{\rm m}^2\right) + a\exp\left(-(A-\bar{A}_{\rm H})/2\sigma_{\rm m}^2\right) \quad (1)$$

where a and $\sigma_{\rm m}$ represent the peak amplitude and standard deviation of the distribution, and $\bar{A}_{\rm L}$ and $\bar{A}_{\rm H}$ are the light- and heavy-fragment peak positions (normalized to add up to the mass of the compound nucleus $A_{\rm c} = \bar{A}_{\rm L} + \bar{A}_{\rm H}$) With the mass asymmetry $\bar{A}_{\rm L} = 80$ and $\bar{A}_{\rm H} = 100$, the value $\sigma_{\rm m} = 4.6$ was deduced.

Present results from fusion–fission reactions (see Fig. 2) show that the shape of the deduced FFs mass distributions remains practically unchanged in the studied range of excitation energies and do not transit to a single-Gaussian shape: a finding which is in contrast with what is experimentally known in other mass regions [8,13,14]. In particular, it is found that the measured mass distributions for ^{180}Hg can also be fitted by Eq. (1) with $\bar{A}_{\rm L} = 79$ and $\bar{A}_{\rm H} = 101$, for all the excitation energies from $E^* = 33.4$ to 65.5 MeV as shown in Fig. 2. [2]

On the other hand, the growing excitation of the compound nucleus is found to show up in the increase of the standard deviation of the Eq. (1). Fig. 3(a) gives the square of the standard deviation,

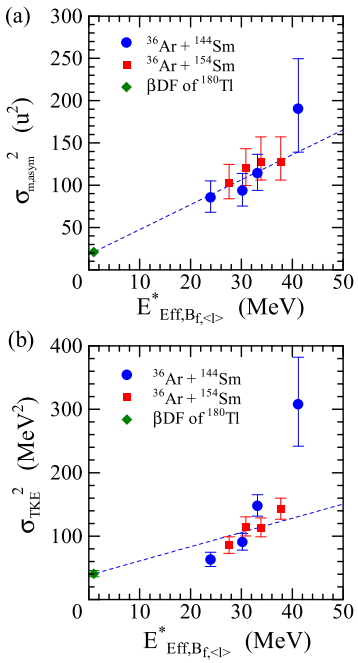

Fig. 3. (Color online.) Standard deviations obtained from the fits of the (a) mass distribution and (b) total kinetic energy distribution, as a function of effective excitation energy above the fission barrier, for the reactions ^{36}Ar + ^{144,154}Sm. Data for ^{180}Hg from the βDF of ^{180}Tl [10,11] are also included. The dashed lines show the results of a linear fit, see text for details.

[1] Comparison of the βDF-MD with the present data should be done with caution, especially at higher beam energies where the MDs are subject of different contributions from the multi-chance fission. For a deeper understanding of the measured MDs, the latter should be decomposed according to the weight of every fission chance. A multi-chance fission weight estimation made with the statistical code HIVAP [26] has indicated that contribution from different chances to the measured MDs remains negligible throughout the range of measured excitations for ^{180}Hg, whereas for more neutron-rich isotope ^{190}Hg similar statement holds only at two lower excitation energies.

[2] The analysis of the MDs has shown that, for the both studied Hg nuclei, the introduction of a symmetric mode into the fit function Eq. (1) does not improve the fit quality. This however does not exclude the existence of the symmetric mode and its contribution to the measured data, especially at higher excitation energies.

$\sigma^2_{\mathrm{m,asym}}$, obtained in the analysis. The plotted values are corrected for the experimental mass resolution $\sigma_{\mathrm{m,exp}}$, with the expression $\sigma^2_{\mathrm{m,asym}} = \sigma^2_{\mathrm{m}} - \sigma^2_{\mathrm{m,exp}}$ except for the data point from the βDF of ^{180}Tl.

Following the prescription made by Itkis [6,7], we introduce the so-called "effective excitation energy $E^*_{\mathrm{Eff},B_{\mathrm{f},\langle l\rangle}}$" which is the excitation energy of a nucleus measured from the top of the angular-momentum-dependent fission barrier, corrected for the rotational energy and pre-scission neutron emission ΔE_{eva}, given by the following expression:

$$E^*_{\mathrm{Eff},B_{\mathrm{f},\langle l\rangle}} = E^* - \Delta E_{\mathrm{eva}} - B_{\mathrm{f},\langle l\rangle} \tag{2}$$

The fission barrier for the rotating nucleus, produced in fusion reaction, with an average angular momentum $\langle l\rangle$ was estimated in the following way:

$$B_{\mathrm{f},\langle l\rangle} = B_{\mathrm{f},0} - \Delta B_{\mathrm{f},\langle l\rangle}, \tag{3}$$

where the calculated fission barrier at zero angular momentum $B_{\mathrm{f},0}(^{180}\mathrm{Hg}) = 9.81$ MeV [27]. Reduction of the barrier height due to nuclear rotation $\Delta B_{\mathrm{f},\langle l\rangle}$ was estimated within the framework of the macroscopic model of rotating nuclei [28]. The average spin $\langle l\rangle$ is calculated with the code [29]. Because of possible neutron emission prior to fission, the excitation energy of the fissioning nucleus decreases by ΔE_{eva}. The determination of ΔE_{eva} will be discussed in Section 4. Emission of protons from nuclei prior to fission estimated in statistical calculations with the PACE4 [30] and HIVAP codes [26,31] was found to be of no importance for the ^{190}Hg ($< 1\%$) and small for ^{180}Hg ($< 15\%$); this mode of de-excitation was, hence, not considered in the following.

The data point for ^{180}Hg from the βDF of ^{180}Tl is also shown in Fig. 3(a), where E^*_{max} was set equal to the Q value of the β^+/EC decay, $Q_{\mathrm{EC}}(^{180}\mathrm{Tl}) = 10.8$ MeV [12], which leads to effective excitation energy above the fission barrier of $\sim$1 MeV. The data in Fig. 3(a) are fitted with a linear function constrained to reproduce the value from the βDF of ^{180}Tl; the fit is shown as the dashed line. The increase of the standard deviation of the mass distribution with excitation energy is a well-known trend for nuclei in the actinide region; its interpretation is given, for example, in the framework of the liquid-drop model [32].

The present analysis shows that the FFs mass distributions of ^{180}Hg can be reliably reproduced by Eq. (1) with only a mass-asymmetric fission mode, at least up to excitation energy of $E^* = 65.5$ MeV. The deduced mass asymmetry is comparable to that obtained in the low-energy βDF study.

A similar analysis was done for the reaction ^{36}Ar + ^{154}Sm $\rightarrow$ ^{190}Hg*, measured up to excitation energies of $E^*(^{190}\mathrm{Hg}) = 70.5$ MeV, and the results are shown in Fig. 4. Here again, all measured mass spectra could be represented by Eq. (1), with the mass asymmetry $\bar{A}_{\mathrm{L}}/\bar{A}_{\mathrm{H}} = 83/107$. The standard deviation $\sigma^2_{\mathrm{m,asym}}$ values are shown in Fig. 3(a), where the fission barrier height for ^{190}Hg was set at $B_{\mathrm{f},0} = 15.2$ MeV [27], to calculate the effective excitation energy $E^*_{\mathrm{Eff},B_{\mathrm{f},\langle l\rangle}}$. It can be noted that the $\sigma^2_{\mathrm{m,asym}}$ values for ^{190}Hg agree well with those deduced for ^{180}Hg when plotted as a function of $E^*_{\mathrm{Eff},B_{\mathrm{f},\langle l\rangle}}$.

The total kinetic energy (TKE) delivers information on the Coulomb energy at the scission point. Fig. 5 shows the TKE distributions for the two studied reactions ^{36}Ar + ^{144,154}Sm, obtained at the respective lowest incident beam energies. The TKE distributions are found to be structureless and can therefore be reproduced by a single Gaussian function as shown in the figure. The latter fact can be further considered as a confirmation of a single-mode asymmetric fission of both nuclei, similar to the βDF of ^{180}Tl [10,11].

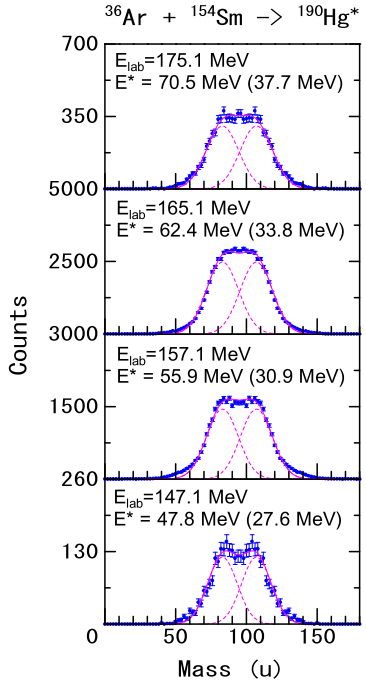

Fig. 4. (Color online.) Same as Fig. 2, but for the reaction ^{36}Ar + ^{154}Sm.

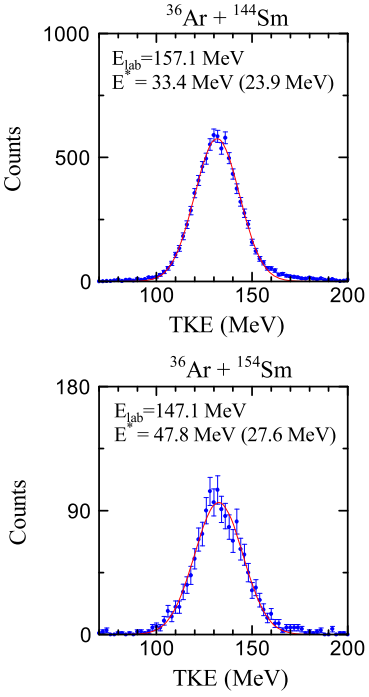

Fig. 5. (Color online.) Total kinetic energies of fragments from fission of ^{180}Hg (upper panel) and ^{190}Hg (lower panel) for $E_{\mathrm{lab}} = 157.1$ and 147.1 MeV, respectively. Continuous lines show the fit of the data with a Gaussian function.

In the present study, the most probable value of TKE(^{180}Hg) = 131.7(10) MeV was obtained. This value agrees well with TKE = 133.2(14) MeV derived in the βDF study of ^{180}Tl [11], but it deviates by $\sim$10 MeV from 142.1 MeV expected from the Viola systematics [33]. From the TKE distribution for ^{190}Hg* measured at $E_{\mathrm{lab}} = 147.1$ MeV (see Fig. 5), a TKE(^{190}Hg) = 132.5(10) MeV was deduced. This value is about 7 MeV lower than TKE = 139.7 MeV expected from the Viola formula [33].

The excitation energy dependence of the standard deviation of the TKE distribution, σ_{TKE}, is shown in Fig. 3(b) for both studied reactions, as a function of $E^*_{\mathrm{Eff},B_{\mathrm{f},\langle l\rangle}}$. The σ_{TKE} values are corrected for the contribution from the experimental resolution $\sigma_{\mathrm{ela+rec}}$. The dashed line is the result of the fit to the data for the ^{180}Hg nucleus only, with the constraint to reproduce the data point from the βDF of ^{180}Tl [10,11]. As seen from Fig. 3(b), the data sets for ^{180,190}Hg agree well within the indicated uncertainties, with the exception of the point at the highest excitation energy of the ^{180}Hg nucleus. Excluding the βDF value from the fit and considering the data from fusion reactions only would give an overall agreement on the two-sigma confidence level.

4. Discussion

Quasifission reactions can potentially be a source of fission events which may to some extent influence the results obtained in the present work. It is known from the literature that no quasifission has been observed in reactions involving spherical nuclei, which is the case for e.g. the ^{48}Ca + ^{144}Sm reaction [34]. As soon as at least one of the nuclei is deformed, the FFs associated with quasifission appear in the reactions with sufficiently large $Z_1 \times Z_2$ (charges of interacting nuclei) values, as found in the reaction ^{48}Ca + ^{154}Sm [34], where the ^{154}Sm nucleus possesses a large static deformation of $(\beta_2, \beta_4) = (0.27, 0.11)$ [35]. Specifically in the ^{48}Ca + ^{154}Sm reaction, the quasifission products are characterized by a large mass-asymmetry $\bar{A}_{\mathrm{L}}/\bar{A}_{\mathrm{H}} = 62/140$, with the probability of the process being inversely proportional to the incident beam energy.

In the present study, a ^{154}Sm target was bombarded with the ^{36}Ar beam. As follows from the measured mass distributions (see Fig. 4), practically no events with extreme mass-asymmetry have been detected, at all incident beam energies. The same holds for the ^{36}Ar + ^{144}Sm reaction. Also, the Gaussian-like TKE distributions for the two studied reactions, ^{36}Ar + ^{144,154}Sm, agree within 1 MeV at the average value, and practically overlaps with the TKE value from the βDF of ^{180}Tl, where quasifission is excluded. We thus conclude that mass-asymmetric splits observed in both reactions are exclusively due to fission from the excited compound nuclei.

As mentioned in Section 3, the initial excitation energy of a fissioning system, E^*, can be reduced by evaporation of neutrons prior to fission. This energy, ΔE_{eva}, was estimated for every incident beam energy. As shown by the earlier systematical studies[36] the pre-sission neutron multiplicities M_{pre} are expected to linearly increase with excitation energy and atomic number of the compound nucleus, according to the expression:

$$M_{\mathrm{pre}} = 0.8\left(\mu_{\mathrm{n}}\left(E^* + \langle Q_{\mathrm{eff}}\rangle_{\mathrm{Zcn}}\right) - M_0\right), \tag{4}$$

A value of $\mu_{\mathrm{n}} = 0.075$ MeV^{-1} is commonly used for nuclei with proton number Z_{CN} ranging from 55 to 120 at excitation energies $E^* < 200$ MeV. For nuclei with $Z_{\mathrm{CN}} = 76$–80, the values for the parameters M_0 and $\langle Q_{\mathrm{eff}}\rangle_{\mathrm{Zcn}}$ were derived to be 2.5 and −5 MeV, respectively. Within the range of studied excitation energies, the neutron emission is expected to change from $M_{\mathrm{pre}} = 0$ to $M_{\mathrm{pre}} = 1.63$ for ^{180}Hg and from $M_{\mathrm{pre}} = 0.57$ to $M_{\mathrm{pre}} = 1.93$ for ^{190}Hg. ΔE_{eva} was then determined from the neutron binding energy and average neutron kinetic energy in the center-of-mass frame calculated with the PACE2 code [30]. The results are summarised in Table 1.

Our new fission data on the extremely proton-rich mercury nuclei offer a new benchmark for theoretical approaches to fission. After the discovery of the asymmetric fission of ^{180}Hg, several theory groups made calculations for the mass distribution for ^{180}Hg and some of the heavier mercury isotopes. Several studies were based on the analysis of the potential-energy surface of the fissioning nucleus derived either in the macroscopic–microscopic approach [17,18], or in the fully-microscopic HFB model [19]. The finite temperature superfluid nuclear density functional theory was applied in [20]. The calculations by the Dubna [21,22] and Saclay [23] groups were based on a modified scission-point model. An interesting, though a somewhat surprising fact was that all the models were able to reproduce reasonably well observed most probable masses for light and heavy FFs from the low-energy fission of ^{180}Hg, despite the variety of the model concepts applied.

Table 1
The mid-target beam energies E_{lab} and respective initial excitation energies E^* for the two studied reactions. The columns from 2 to 5 give the calculated values of the average angular momentum $\langle l\rangle$ ($\hbar$), fission barrier height of a rotating nucleus $B_{\mathrm{f},\langle l\rangle}$ (MeV), neutron multiplicity M_{pre}, loss of excitation energy due to neutron evaporation ΔE_{eva} (MeV). The last column gives the effective intrinsic excitation energy of a fissioning nucleus relative to the height of the fission barrier, $E^*_{\mathrm{Eff},B_{\mathrm{f},\langle l\rangle}}$ (MeV).

E_{lab} (E^*) MeV	$\langle l\rangle$	$B_{\mathrm{f},\langle l\rangle}$	M_{pre}	ΔE_{eva}	$E^*_{\mathrm{Eff},B_{\mathrm{f},\langle l\rangle}}$
^{36}Ar + ^{144}Sm → ^{180}Hg*					
157.1 (33.4)	9.6	9.5	0.00	0.0	23.9
165.1 (39.8)	20.5	8.4	0.09	1.2	30.2
175.1 (47.8)	30.0	6.9	0.57	7.8	33.1
197.2 (65.5)	46.8	3.4	1.63	21.0	41.2
^{36}Ar + ^{154}Sm → ^{190}Hg*					
147.1 (47.8)	22.9	13.4	0.57	6.8	27.6
157.1 (55.9)	29.3	12.4	1.05	12.6	30.9
165.1 (62.4)	31.0	12.1	1.44	16.5	33.8
175.1 (70.5)	37.5	10.8	1.93	22.0	37.7

Concerning the MDs dependence on the excitation energy, the theory works are less numerous. As it has been shown experimentally (see Section 3), the mass asymmetry in fission of ^{180,190}Hg remains constant through the measured energy ranges $E^*_{\mathrm{Eff},B_{\mathrm{f},\langle l\rangle}}(^{180}\mathrm{Hg}) = 23.9$–$41.2$ MeV and $E^*_{\mathrm{Eff},B_{\mathrm{f},\langle l\rangle}}(^{190}\mathrm{Hg}) = 27.6$–$37.7$ MeV. This finding is corroborated by the calculations of the FFs mass distribution for ^{180}Hg [17], which predicted the mass asymmetry to vary little with excitation energy and to stay nearly constant at $\bar{A}_{\mathrm{L}}/\bar{A}_{\mathrm{H}}(^{180}\mathrm{Hg}) \approx 74/106$ in the range of $E^* = (B_{\mathrm{f},0} + 2)$ MeV to 40 MeV. Even if absolute values of $\bar{A}_{\mathrm{L}}/\bar{A}_{\mathrm{H}}$ show some deviation with measured data, the trend of the calculation is consistent with the experiment. For ^{190}Hg, a nearly constant mass asymmetry of $\bar{A}_{\mathrm{L}}/\bar{A}_{\mathrm{H}} = 79/111$ is predicted in the range of energies $E^* = (B_{\mathrm{f},0} + 2)$ MeV to 40 MeV [17,37]. The experiment gives the mass asymmetry $\bar{A}_{\mathrm{L}}/\bar{A}_{\mathrm{H}}(^{190}\mathrm{Hg}) = 83/107 = 0.776$, which is close to the calculated one. The observed asymmetry in fragment masses from fission of both nuclei is similar ($\bar{A}_{\mathrm{L}}/\bar{A}_{\mathrm{H}} \approx 0.78$)

Effects of nuclear rotation on the mass-asymmetry degree of freedom were also examined in the above-mentioned model calculations [17,37]. The rotation was found to have only minor effects on the fragment-mass asymmetry up to spin value as high as 40$\hbar$. As shown in Table 1, the average angular momentum $\langle l\rangle$ of the systems studied in this experiment is hardly exceeding this value. Therefore, the nuclear rotation cannot be considered as the factor responsible for the mass division.

Fission mass asymmetries of ^{180,198}Hg and their excitation energy dependence were recently studied by calculating the potential energy with a finite-temperature superfluid nuclear density functional theory, see Fig. 1 of [20]. The authors were able to calculate the total shell correction energy along the symmetric and asymmetric-fission paths in ^{174,180,198}Hg, and they concluded that "... the preference for the asymmetric pathway in ^{180}Hg is driven by shell effects in pre-scission configuration." Important for the present study, the calculated trend of lowering the fission barrier as a function of the excitation energy (see Fig. 4 of [20]) was found

to be very gentle, thus leading to asymmetric fission at least up to $E^*(^{180}\mathrm{Hg}) = 30$ MeV, which was the maximum excitation energy used in the calculations for their Fig. 5.

This study [20] could also correctly reproduce the transition to a more symmetric fission mass split for ^{198}Hg, observed earlier in [6]. The ^{190}Hg nucleus, studied in the present work and situated mid-way between ^{180}Hg and ^{198}Hg, shows a mass-asymmetric fission up to high excitation energy, which is similar to ^{180}Hg, but differs from that of ^{198}Hg. It would be interesting to see if the theory can reproduce this observation as well.

5. Conclusions

Fission-fragment mass and total kinetic-energy distributions were determined for the excited ^{180,190}Hg nuclei formed in fusion reactions of ^{36}Ar + ^{144}Sm and ^{36}Ar + ^{154}Sm. The data were obtained in the effective excitation energy range from the top of the fission barrier of 24–41 MeV and 27–38 MeV for ^{180}Hg and ^{190}Hg, respectively. The mass distributions for both Hg isotopes could be well reproduced with a single asymmetric fission mode, and the mass asymmetry was found to be constant throughout the measured excitation energy range, for both compound systems. For ^{180}Hg, the measured mass-asymmetry $\bar{A}_\mathrm{L}/\bar{A}_\mathrm{H} = 79/101$ agrees well with that known from the low-energy β^+/EC delayed fission of ^{180}Tl. For ^{190}Hg, the mass-asymmetry was found to be $\bar{A}_\mathrm{L}/\bar{A}_\mathrm{H} = 83/107$, having almost the same value ≈ 0.78 as for ^{180}Hg. The similarity of FFs properties in the studied reactions is seen in the behavior of the width of the mass and TKE distributions, if scaled with the effective intrinsic excitation energy on the top of the fission barrier.

The measured mass asymmetries were compared with several available model calculations. The theory predicts mainly mass-asymmetric fission of excited ^{180,190}Hg nuclei, with the mass-asymmetry showing minor changes with excitation energy; we find these expectations in overall agreement with the experiment. This is a remarkable result, taking into consideration very different model assumptions. Assuming that the mass asymmetry in fission is governed by microscopic shell effects, one comes to the conclusion that, in the studied cases of the ^{180,190}Hg isotopes, these shell effects should be robust at least up to initial excitation energy of a nucleus up to about $E^*_{\mathrm{Eff},B_{\mathrm{f},(l)}} = 40$ MeV. This conjecture is in sharp contrast to what is known in other regions, e.g. for fission of the heavy actinides, where shell effects are quickly washed out with increase of excitation energy. To conclude, we strongly believe that it is important to extend such studies, both experimental and theoretical, to other neutron-deficient nuclei in this interesting and hardly-studied region, as far as fission is concerned.

Acknowledgements

The authors thank the staff of the JAEA-tandem facility for the beam operation and the GSI target laboratory for preparation of the Sm targets. Special thanks for extensive discussions of calculated FFs mass distributions are due to Drs. P. Möller and J. Randrup. Support from the University of Bordeaux (France) in the framework of the IdEx program is gratefully acknowledged. The work was supported by the Science and Technology Facilities Council (STFC), United Kingdom, and by the FWO-Vlaanderen, Belgium.

References

[1] B.D. Wilkins, E.P. Steinberg, R.R. Chasman, Phys. Rev. C 14 (1976) 1832.
[2] A.W. Fairhall, Phys. Rev. 102 (1956) 1335.
[3] R.C. Jensen, A.W. Fairhall, Phys. Rev. 109 (1958) 942.
[4] E. Konecny, et al., Nucl. Phys. A 139 (1969) 513.
[5] K.-H. Schmidt, et al., Nucl. Phys. A 665 (2000) 221.
[6] M.G. Itkis, et al., Sov. J. Nucl. Phys. 52 (1990) 601.
[7] M.G. Itkis, et al., Sov. J. Nucl. Phys. 53 (1991) 757.
[8] M.G. Itkis, et al., Sov. J. Part. Nucl. 19 (1988) 301.
[9] S.I. Mulgin, K.-H. Schmidt, A. Grewe, S.V. Zhdanov, Nucl. Phys. A 640 (1998) 375.
[10] A.N. Andreyev, et al., Phys. Rev. Lett. 105 (2010) 252502.
[11] J. Elseviers, et al., Phys. Rev. C 88 (2013) 044321.
[12] G. Audi, et al., Nucl. Phys. A 729 (2003) 337.
[13] I.F. Croall, et al., Nucl. Phys. A 125 (1969) 402.
[14] D.G. Perry, A.W. Fairhall, Phys. Rev. C 4 (1971) 977.
[15] J. Randrup, et al., Phys. Rev. C 88 (2013) 064606.
[16] J. Randrup, P. Möller, Phys. Rev. Lett. 106 (2011) 132503.
[17] P. Möller, J. Randrup, A. Sierk, Phys. Rev. C 85 (2012) 024306.
[18] T. Ichikawa, et al., Phys. Rev. C 86 (2012) 024610.
[19] M. Warda, A. Staszczak, W. Nazarewicz, Phys. Rev. C 86 (2012) 024601.
[20] J.D. McDonnell, et al., Phys. Rev. C 90 (2014) 021302(R).
[21] A.V. Andreev, et al., Phys. Rev. C 86 (2012) 044315.
[22] A.V. Andreev, et al., Phys. Rev. C 88 (2013) 047604.
[23] S. Panebianco, et al., Phys. Rev. C 86 (2012) 064601.
[24] K. Nishio, et al., Phys. Rev. C 77 (2008) 064607.
[25] http://www.srim.org/SRIM/SRIMLEGL.htm.
[26] W. Reisdorf, M. Schädel, Z. Phys. A 343 (1992) 47.
[27] P. Möller, et al., Phys. Rev. C 91 (2015) 024310.
[28] A.J. Sierk, Phys. Rev. C 33 (1986) 2039.
[29] K. Hagino, et al., Comput. Phys. Commun. 123 (1999) 143.
[30] A. Gavron, Phys. Rev. C 21 (1980) 230.
[31] A.N. Andreyev, et al., Phys. Rev. C 72 (2005) 014612.
[32] J.R. Nix, Nucl. Phys. A 130 (1969) 241.
[33] V.E. Viola, et al., Phys. Rev. C 31 (1985) 1550.
[34] G.N. Knyazheva, et al., Phys. Rev. C 75 (2007) 064602.
[35] P. Möller, et al., At. Data Nucl. Data Tables 59 (1995) 185.
[36] D. Hilscher, H. Rossner, Ann. Phys. Fr. 17 (1992) 471.
[37] T. Ichikawa, P. Möller, private communication.